DOI: 10.1002/chem.201000003

Synthesis, Structure and Molecular Recognition of Functionalised Tetraoxacalix[2]arene[2]triazines

Qi-Qiang Wang,[a] De-Xian Wang,*[a] Hai-Bo Yang,[a] Zhi-Tang Huang,[a] and Mei-Xiang Wang*[a, b]

Abstract: Functionalised dialkoxy-substituted tetraoxacalix[2]arene[2]triazine macrocycles **6** have been readily synthesised by the fragment coupling approach using methyl 3,5-dihydroxy-4-alkoxybenzoates and cyanuric chloride as the starting materials under very mild conditions. $AlCl_3$-mediated deallylation and debenzylation reactions afforded the lower-rim dihydroxy-substituted tetraoxacalix[2]arene[2]triazine derivatives **11** and **13** in good yields. Although dialkoxy-substituted tetraoxacalix[2]arene[2]triazine macrocycles are fluxional in solution on the NMR spectroscopy timescale, they adopt a symmetric or slightly distorted 1,3-alternate conformation with the bridging oxygen atoms conjugated with the triazine rings. The dihydroxylated tetraoxacalix[2]arene[2]triazine **13b**, which gives a mixture of monomer and dimer in solution according to a diffusion NMR spectroscopy study, adopts a 1,3-alternate conformation and forms a cyclic tetrameric assembly in the solid state due to the formation of intermolecular hydrogen-bonding networks. This dihydroxylated macrocyclic host molecule, a hydrogen-bond donor macrocycle with a V-shaped cleft, interacts with 2,2′-bipyridine, 4,4′-bipyridine and 1,10-phenanthroline guests. Although in solution they form the corresponding 1:1 complexes with binding constants ranging from 37.7 to 213 M^{-1}, 2:2 host–guest complexes were observed in the crystalline state. Hydrogen-bonding interactions, along with other non-covalent interactions, such as lone-pair-electron–π and C–H···π interactions, were found to be the driving force for the formation of host–guest complexes.

Keywords: calixarenes · host–guest systems · hydrogen bonds · molecular recognition · structure elucidation

Introduction

The design and synthesis of novel and functional macrocyclic molecules have always been one of the driving forces for promoting major advances in supramolecular science. This has been demonstrated through the synthesis of well-known crown ethers,[1] spherands[2] and cryptands.[3] A recent example is the extensive study of the supramolecular chemistry of calixarenes[4] following Gutsche's pioneering work on the synthesis and structural elucidation of calix[*n*]arenes.[5] Because of their easy availability, unique conformational and cavity structures, and powerful recognition properties, calix[*n*]arenes have become classic macrocyclic molecules.[4]

Along with the advances in the field of calix[*n*]arenes, heterocalixaromatics,[6–10] heteroatom-bridged calix(hetero)arenes, have emerged as a novel type of macrocyclic host molecule in supramolecular chemistry. Owing to the bridging heteroatoms, such as nitrogen, oxygen and sulfur, which can adopt different electronic configurations and form different degrees of conjugation with their neighbouring aromatic rings, heterocalixaromatics are able to form fine-tuneable conformation and cavity structures that interact with various guest species. For example, azacalix[4]pyridine forms coordination complexes selectively with transition- and heavy-metal cations.[7f,o] By forming intermolecular hydrogen bonds, azacalix[4]pyridine forms a variety of com-

[a] Q.-Q. Wang, Dr. D.-X. Wang, H.-B. Yang, Prof. Z.-T. Huang, Prof. Dr. M.-X. Wang
Beijing National Laboratory for Molecular Sciences
CAS Key Laboratory of Molecular Recognition and Function
Institute of Chemistry, Chinese Academy of Sciences
Beijing 100190 (P.R. China)
Fax: (+86) 10-62564723
E-mail: wangmx@tsinghua.edu.cn
mxwang@iccas.ac.cn

[b] Prof. Dr. M.-X. Wang
The Key Laboratory of Bioorganic Phosphorus Chemistry & Chemical Biology (Ministry of Education), Department of Chemistry
Tsinghua University, Beijing 100084 (P.R. China)

Supporting information for this article is available on the WWW under http://dx.doi.org/10.1002/chem.201000003.

plexes with aliphatic and aromatic monoalcohols and diols.[7l] The large macrocyclic homologues, azacalix[*n*]pyridines ($n=5$–10), exhibit a strong binding ability towards fullerenes such as C_{60} and C_{70}.[7e,m,n] Very recently, tetraoxacalix[2]arene[2]triazines have been reported to recognise halides through the formation of anion–π interactions.[11]

Although a number of heterocalixaromatics have been prepared in recent years, functionalised heterocalixaromatics with functional groups for molecular recognition and assembly are very rare. We previously synthesised tetraoxacalix[2]arene[2]triazines that contain metal-ion-chelating ligands, azacrown ethers and fluorescence moieties on the larger rim.[12] Dehaen and co-workers[13] have also reported the larger-rim functionalisation of tetraoxacalix[2]arene[2]-pyrimidine with a benzocrown ether and L-cysteine ethyl ester groups. To explore the applications of heterocalixaromatics in molecular recognition and molecular assembly, the construction of functional macrocycles is highly desirable. Because the tetraoxacalix[2]arene[2]triazine macrocycle generally adopts a 1,3-alternate conformation with two benzene rings nearly face-to-face parallel and two triazine rings tending to an edge-to-edge orientation,[8a] we envisioned that the introduction of hydroxy groups on to the benzene rings would give rise to a functionalised cavity. We report herein the synthesis and structures of smaller-rim dihydroxy-substituted tetraoxacalix[2]arene[2]triazine derivatives. The resulting macrocyclic molecules provide a unique V-shaped cavity that forms interesting complexes with 2,2′-bipyridine, 4,4′-bipyridine and 1,10-phenanthroline through hydrogen bonding and C–H···π and π–π interactions.

Results and Discussion

Synthesis: We have previously shown that the fragment coupling approach is generally efficient and practical for the synthesis of diverse heterocalixaromatics. We initiated our study with the synthesis of 2,6-bis(4,6-dichloro-1,3,5-triazin-2-yloxy)phenol, or "trimer" **3**, by the reaction of 1,2,3-trihydroxybenzene (**1a**) or the methyl ester of gallic acid (**1b**) with cyanuric chloride (**2**). However, a mixture of oligomers was produced from the reaction instead of the target molecule **3** (Scheme S1 in the Supporting Information).

We then attempted the reactions of **4a–c**, gallic acid ester derivatives with an allyl, benzyl and methyl protecting group, respectively, on the 4-hydroxy group. In the presence of diisopropylethylamine as an acid scavenger, all reactants **4a–c** readily underwent nucleophilic aromatic substitution reactions with cyanuric chloride (**2**; 2 equiv) at 0 °C to afford the corresponding intermediates **5a–c** in yields ranging from 74 to 84%. A 3+1 macrocyclic cyclisation was then performed. Treatment of the linear trimers **5a–c** with **4a–c** at room temperature led to the formation of tetraoxacalix[2]arene[2]triazine derivatives **6a–c** in moderate yields. Surprisingly, the reaction between **5a** and **4a** gave hexaoxacalix[3]arene[3]triazine **7a** in a yield of 14% in addition to **6a**. A similar larger macrocyclic ring analogue **7c** was also obtained in 10% yield from the reaction of **5c** with **4c** (Scheme 1).

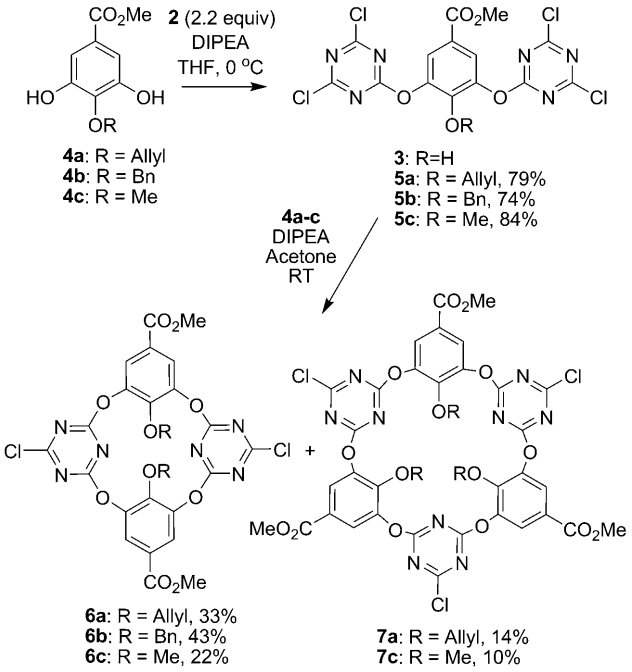

Scheme 1. Synthesis of tetraoxacalix[2]arene[2]triazine derivatives **6**.

The formation of hexaoxacalix[3]arene[3]triazines **7a,c** from the 3+1 fragment coupling reactions between **5a,c** and **4a,c** was intriguing. A plausible mechanism could involve the formation of intermediate **8** (Scheme 2) from the

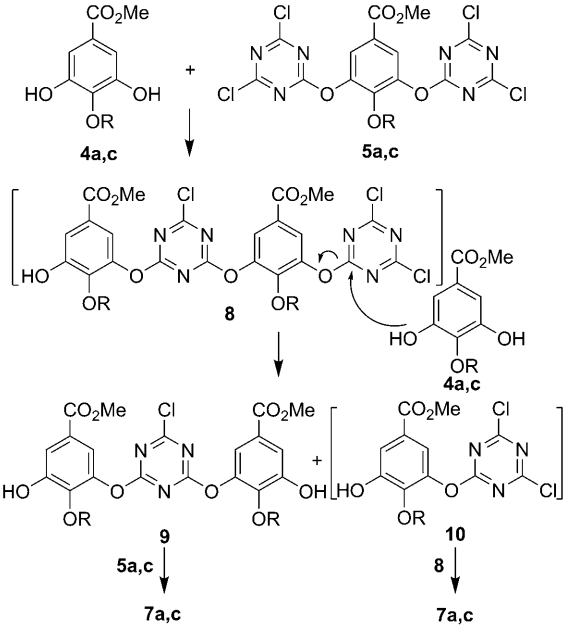

Scheme 2. Plausible reaction pathways for the formation of **7a,c**.

reaction between **4** and **5**. Prior to intramolecular cyclisation, which afforded tetraoxacalix[2]arene[2]triazine **6**, the linear tetramer **8** was most probably cleaved by **4a** and **4c** to produce a linear trimer intermediate **9** and a dimer intermediate **10**. Both a 3+3 fragment coupling of **9** with **5** and a 2+4 fragment coupling of **10** with **8** would lead to hexaoxacalix[3]arene[3]triazines **7**. The cleavage of linear tetramer **8** by **4a** and **4c** is most likely due to the high reactivity of the C–O bond of the dichloro-substituted triazine ring. Note that, because of the steric hindrance of methyl 4-benzyloxy-3,5-dihydroxybenzoate (**4b**), no effective nucleophilic aromatic attack at **8** took place. Therefore, no hexaoxacalix[3]arene[3]triazine product was yielded.

To synthesise the target lower-rim dihydroxylated tetraoxacalix[2]arene[2]triazine, compounds **6a** and **6b** were subjected to deprotection. However, no deallylation reaction was achieved by using a number of documented methods. Catalytic hydrogenolysis of **6b** under various conditions did not remove the benzyl group either. We finally performed the deprotection of **6a** and **6b** with an excess amount of $AlCl_3$ in dry toluene; both allyl and benzyl groups were cleaved efficiently at ambient temperature. Under the reaction conditions, the two triazine rings were also arylated by toluene in a Friedel–Crafts reaction. The dihydroxy-substituted tetraoxacalix[2]arene[2]triazine **11** was obtained in yields of 75 (R = Bn) and 89% (R = allyl; Scheme 3).

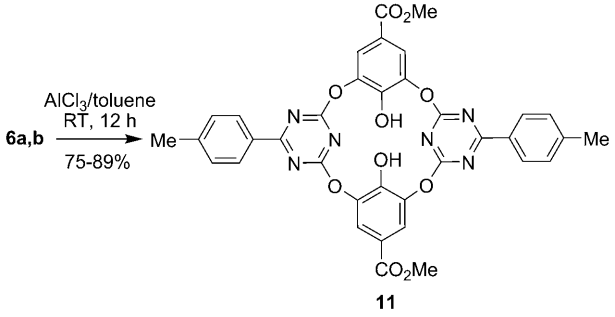

Scheme 3. Deallylation of **6a** and debenzylation of **6b**.

To examine the generality of the $AlCl_3$-mediated deprotection reaction and also to prepare other lower-rim dihydroxy-substituted tetraoxacalix[2]arene[2]triazine analogues, *O*-benzylated tetraoxacalix[2]arene[2]triazine **12a** was synthesised from the reaction of **6b** with di-*n*-propylamine in a yield of 86%. Treatment of **12a** with $AlCl_3$ in dry toluene at room temperature for 30 min gave the desired product **13a** in a quantitative yield. The debenzylation reaction proceeded equally efficiently for the *tert*-butyl-substituted substrate **12b**[8k] to afford the corresponding dihydroxylated tetraoxacalix[2]arene[2]triazine **13b** in a yield of 91% (Scheme 4). It is worth mentioning that $AlCl_3$ is used to remove *tert*-butyl groups from conventional calix[*n*]arenes derived from 4-*tert*-butylphenol.[14]

Note that the selective removal of one of the two benzyl groups in **12** met with failure under the conditions using

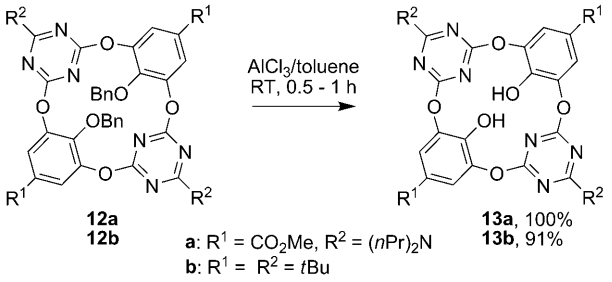

Scheme 4. Synthesis of lower-rim dihydroxylated tetraoxacalix[2]arene[2]triazines **13**.

$AlCl_3$. To synthesise tetraoxacalix[2]arene[2]triazine with one hydroxy group at the lower rim, we studied the selective O-benzylation of **13a**. In the presence of K_2CO_3 in acetone, compound **13a** underwent benzylation with benzyl bromide at ambient temperature to give mono- and dibenzylated products **14** and **12a** in yields of 22 and 30%, respectively (Scheme 5). The use of an excess amount of benzyl bromide (4 equiv) and K_2CO_3 (4 equiv) afforded **12a** as the sole product in a yield of 83%. The chemical yield of **12a** was further improved to 92% when the reaction was carried out in acetone at reflux. The easy benzylation of the hydroxy group of **13a** implies a convenient route to tetraoxacalix[2]arene[2]triazines functionalised on the lower rim.

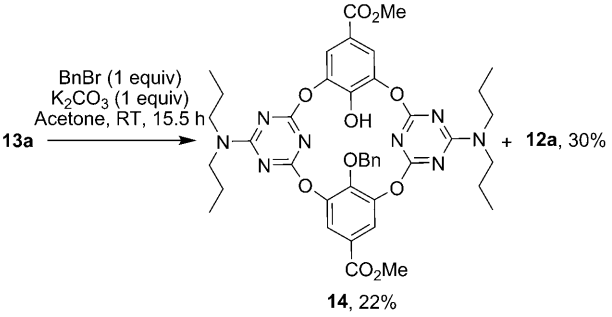

Scheme 5. Synthesis of lower-rim monohydroxylated tetraoxacalix[2]arene[2]triazine **14**.

Structure elucidation: All of the functionalised tetraoxacalix[2]arene[2]triazine products synthesised were crystalline compounds. High-quality single crystals of compounds **6a**, **6b**,[8k] **7a** and **13b** were obtained by slow evaporation of the solvent from their solutions. X-ray diffraction analysis (Table 1) thus allowed us to examine their structures in the solid state. As we reported previously,[8a] the parent tetraoxacalix[2]arene[2]triazine exists as a 1,3-alternate conformer with C_{2v} symmetry. The bridging oxygen atoms tend to conjugate with the triazine rings rather than the benzene rings. As a result, the two benzene rings are almost face-to-face parallel, whereas the two triazine rings tend to adopt an edge-to-edge orientation. The introduction of functional groups such as ester and alkoxy substituents on the benzene rings led to a slight distortion of the 1,3-alternate conforma-

Table 1. X-ray crystallographic data for the macrocyclic host molecules and their complexes.

Compound	**6a**	**7a**	**13b**·0.25 hexane·H_2O	**14**	**13b**·1,10-phen	**13b**·4,4′-bipy	**13b**·2,2′-bipy
empirical formula	$C_{28}H_{20}Cl_2N_6O_{10}$	$C_{42}H_{30}Cl_3N_9O_{15}$	$C_{35.5}H_{47.5}N_6O_7$	$C_{41}H_{46}N_8O_{10}$	$C_{46}H_{50}N_8O_6$	$C_{44}H_{50}N_8O_6$	$C_{44}H_{50}N_8O_6$
M_r	671.40	1007.10	670.30	810.86	810.94	786.92	786.92
crystal size [mm^3]	0.30×0.20×0.16	0.45×0.35×0.10	0.20×0.18×0.16	0.30×0.30×0.25	0.23×0.23×0.18	0.14×0.09×0.08	0.24×0.22×0.14
crystal system	triclinic	monoclinic	tetragonal	monoclinic	monoclinic	monoclinic	monoclinic
space group	$P\bar{1}$	$P2_1/n$	$P4/n$	$C2/c$	$P2_1/n$	$P21/c$	$P121/c1$
a [Å]	9.224(3)	12.039(2)	23.6877(12)	12.979(3)	10.378(2)	10.626(2)	10.7382(5)
b [Å]	12.949(4)	15.317(3)	23.6877(12)	24.289(5)	17.795(4)	18.268(4)	17.8451(7)
c [Å]	14.548(5)	24.823(5)	13.3531(8)	26.134(5)	24.280(57)	22.502(4)	22.4369(11)
α [°]	66.660(5)	90.00	90.00	90.00	90.00	90.00	90.00
β [°]	85.287(5)	90.36(3)	90.00	101.16(3)	102.17(3)	96.46(3)	97.868(2)
γ [°]	72.483(5)	90.00	90.00	90.00	90.00	90.00	90.00
V [Å^3]	1520.1(8)	4577.3(15)	7492.5(7)	8083(3)	4382.9(15)	4340.3(15)	4259.0(3)
d [g cm^{-3}]	1.467	1.461	1.188	1.333	1.229	1.204	1.227
Z	2	4	8	8	4	4	4
T [K]	293(2)	173(2)	113(2)	293(2)	173(2)	293(2)	113(2)
R factor [$I>2\sigma(I)$]	0.0535	0.1063	0.0775	0.1050	0.0806	0.1339	0.0627
R factor (all data)	0.0974	0.1178	0.0840	0.1734	0.0954	0.2668	0.0773
quality of fit	1.017	1.185	1.260	1.473	1.125	1.115	1.116
CCDC no.	759599	759852	759949	759950	759951	759952	759953

tions of the products **6a** and **6b** (Figures 1 and 2), which indicates that the tetraoxacalix[2]arene[2]triazine macrocycle in general prefers a 1,3-alternate conformation. However,

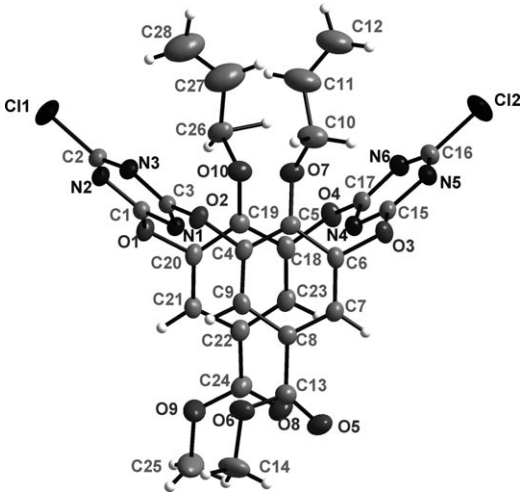

Figure 1. Molecular structure of **6a** (side view). Selected bond lengths [Å]: C1–O1 1.339, O1–C20 1.408, C3–O2 1.334, O2–C4 1.408, C15–O3 1.344, O3–C6 1.408, C17–O4 1.332, O4–C18 1.407. Distances of the upper and lower rims of **6a** [Å]: C8···C22 5.579, C5···C19 4.350, C2···C16 8.515, N1···N4 4.572.

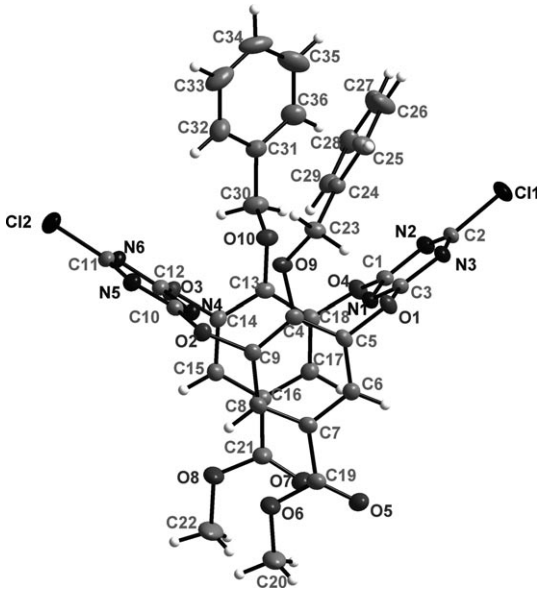

Figure 2. Molecular structure of **6b** (side view). Selected bond lengths [Å]: C1–O4 1.340, O4–C18 1.406, C3–O1 1.339, O1–C5 1.410, C10–O2 1.342, O2–C9 1.412, C12–O3 1.343, O3–C14 1.410. Distances of the upper and lower rims of **6b** [Å]: C7···C16 4.647, C4···C13 4.510, C2···C11 8.911, N1···N4 4.599.

the cavity of the macrocycles **6a** and **6b** differ considerably. For example, whereas the upper rim distance of **6a** ($d_{C8–C22}$) is 5.579 Å, a much shorter distance was observed for **6b** ($d_{C7–C16}$ = 4.647 Å) . Note also that one of the benzyl groups on the lower rim in **6b** tends to locate in the cleft formed by the triazine rings (Figure 2). In the solid state of **6a**, each macrocycle interacts with another two molecules through π–π stacking interactions between triazine rings and by weak hydrogen-bonding interactions between triazine nitrogen atoms and hydrogen atoms of the benzene rings yielding an infinite one-dimensional assembly (Figure S1 in the Supporting Information). Macrocycle **6b** forms a similar one-dimensional assembly in the crystal structure. In contrast to **6a**, however, intermolecular hydrogen bonds between the chlorine atoms on the triazine rings and hydrogen atoms on the benzene rings were observed in addition to π–π stacking interactions between triazine rings (Figure S2 in the Supporting Information).

Hexaoxacalix[3]arene[3]triazine **7a** adopts a 1,3,5-alternate conformation in the solid state (Figure 3). On the basis of the bond lengths and angles of the bridging oxygen

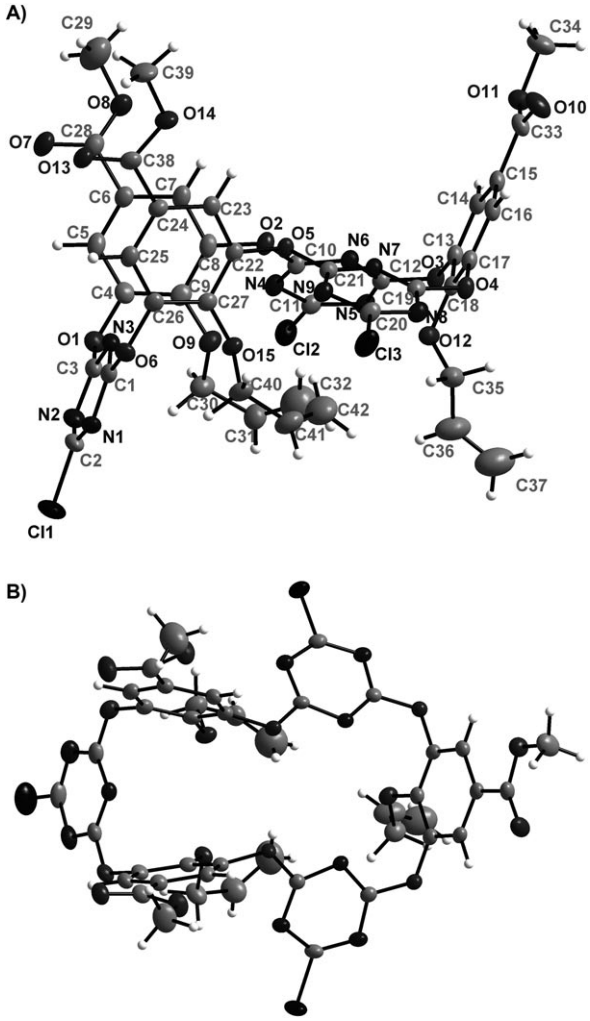

Figure 3. Molecular structure of **7a**: A) side view and B) top view. Selected bond lengths [Å]: C3–O1 1.332, O1–C4 1.404, C1–O6 1.330, O6–C26 1.417, C21–O5 1.332, O5–C22 1.408, C19–O4 1.354, O4–C17 1.405, C12–O3, 1.346, O3–C13 1.412, C10–O2 1.328, O2–C8 1.413. Distances of the upper and lower rims of **7a** [Å]: C6···C24 5.509, C6···C15 9.233, C24···C15 9.360, C9···C27 4.113, C9···C18 6.696, C27···C18 6.784, C2···C20 8.627, C2···C11 8.490, C11···C20 8.690, N3···N7 6.773, N3···N6 6.873, N6···N7 3.995.

atoms, each of the triazine rings is conjugated with the attaching oxygen atoms. The benzene moieties, on the other hand, are not conjugated with the bridging oxygen atoms. The cavity of hexaoxacalix[3]arene[3]triazine **7a** is constructed of a cyclic array of three isolated benzene rings and three bis-oxa-conjugated triazine segments in a 1,3,5-alternate manner. Similarly to **6a** and **6b**, hexaoxacalix[3]arene[3]triazine **7a** also yields an infinite one-dimensional assembly through intermolecular π–π stacking effects between triazine rings (Figure S3 in the Supporting Information).

Although dihydroxylated tetraoxacalix[2]arene[2]triazine **13b** adopts a very slightly twisted 1,3-alternate conformation (Figure 4) similar to that of compounds **6a** and **6b**, the two

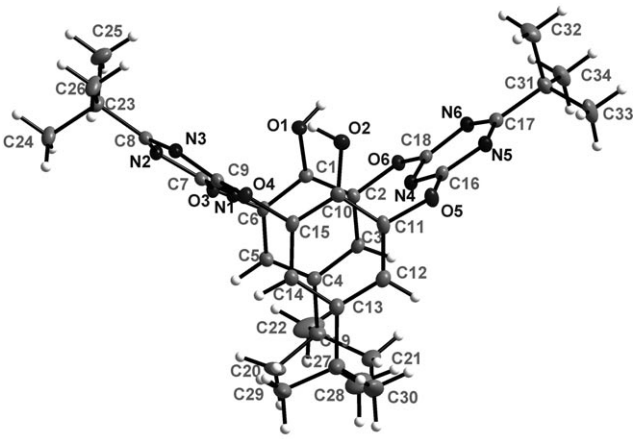

Figure 4. Molecular structure of **13b** (side view). Selected bond lengths [Å]: C7–O3 1.336, O3–C6 1.405, C9–O4 1.353, O4–C15 1.416, C16–O5 1.345, O5–C11 1.415, C18–O6 1.347, O6–C2 1.420. Distances of the upper and lower rims of **13b** [Å]: C4···C13 5.460, C1···C10 4.368, C8···C17 9.022, N1···N4 4.579.

hydroxy groups on the lower rim form different hydrogen bonds intra- and intermolecularly to give an interesting two-dimensional assembly in the solid state. As shown in Figure 5 (top), one of the hydroxy groups (O^A1) of the macrocyclic molecule A forms an intermolecular hydrogen bond with triazine nitrogen N^B2 of the neighbouring macrocycle B, whereas the triazine nitrogen N^A2 of macrocycle A forms a hydrogen bond with the hydroxy group O^D1 of molecule D. Through the formation of four such intermolecular hydrogen bonds between macrocyclic molecules A–D in a cyclic array, a hydrogen-bonded tetrameric structure is obtained. Note that the distance between O^A1 and N^A1 within one macrocycle is 3.028 Å, which suggests a weak intramolecular hydrogen bond between them. The other hydroxy group (O^A2) was found to hydrogen bond with a water molecule (O7) (Figure 5, bottom), which in turn forms a hydrogen bond with triazine nitrogen N^A3. Moreover, the water molecule O7 and the triazine nitrogen of the adjacent macrocycle also forms a hydrogen bond. In other words, two water molecules served as the bridges to connect two tetramers through hydrogen-bonding interactions (Figure 5). As a consequence, one tetramer assembly is linked to another four tetrameric units through hydrogen-bonding networks (see Figure S4 in the Supporting Information).

Compounds **6a**, **6b**, **7a** and **13b** might not retain their solid-state structures in solution. This was evidenced by the NMR spectra, which gave only one set of signals for each of the macrocyclic compounds. These results are in agreement with previous observations[6] and indicate the fluxionality of the macrocycles in solution on the NMR spectroscopy timescale. ^{1}H NMR spectra of **13b** were recorded at various concentrations to shed light on its association behaviour in solu-

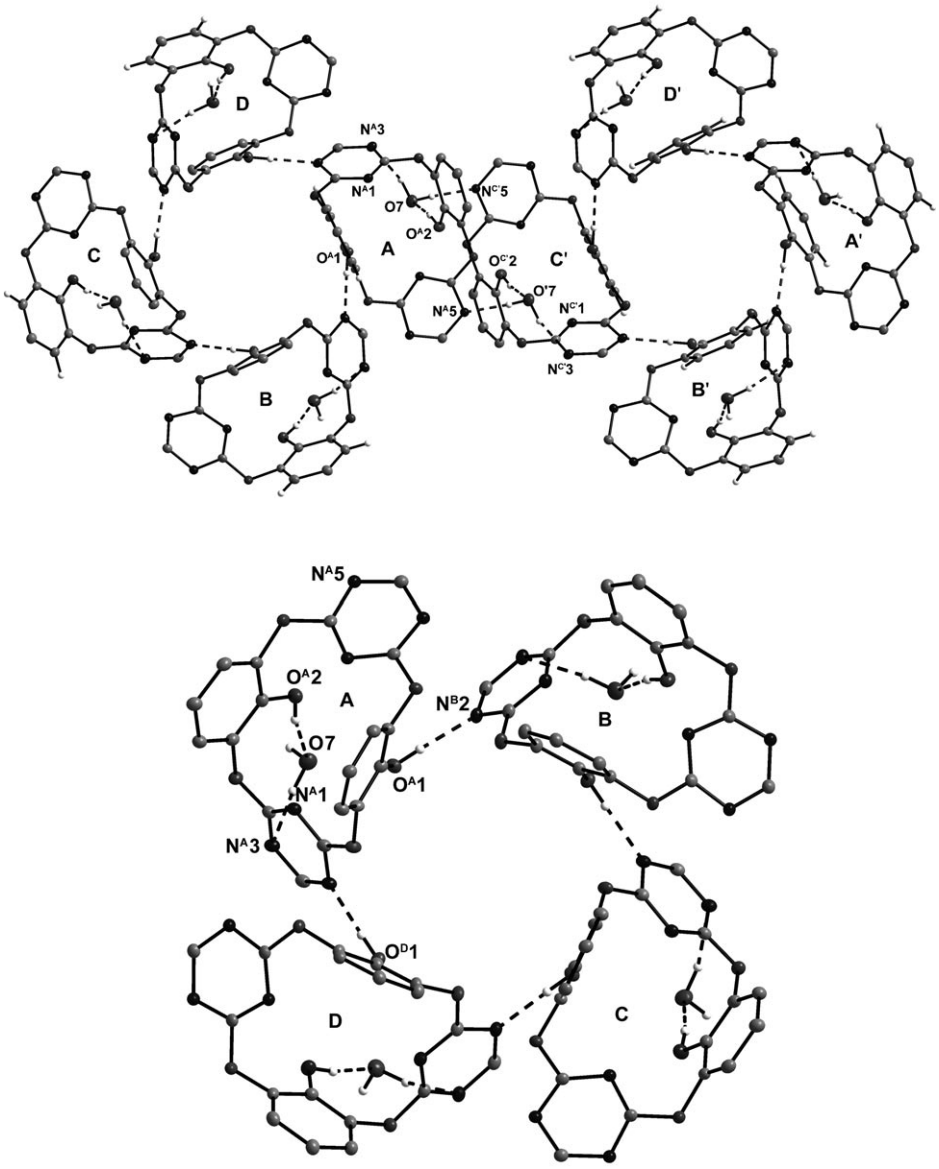

Figure 5. Tetrameric **13b** with a square cavity self-assembled through intermolecular hydrogen bonds (*tert*-butyl groups have been omitted for clarity). Selected hydrogen-bonding distances [Å]: O1···N2 2.809, O2···O7 2.712, O7···N3 2.980, O7···N5 2.875, O1···N3 3.028. Selected hydrogen-bonding angles [°]: O1–H···N2 167.8, O2–H···O7 164.3, O7–H···N3 149.7, O7–H···N5 167.2.

tion. As illustrated in Figure S6 in the Supporting Information, when the concentration of **13b** was increased from 3.17×10^{-3} to 2.67×10^{-2} M, the proton signal of the hydroxy groups was shifted downfield accompanied by a broadening of the peak. This suggests that the hydroxy groups form intermolecular hydrogen bonds. We studied the self-aggregation behaviour of **13b** in solution by NMR diffusion measurements (Figure S7 in the Supporting Information). We first measured the diffusion coefficient of **13b** in a mixture of $CDCl_3$ and CD_3OD (92:8, v/v). As a protonic solvent, methanol is able to form hydrogen bonds with a polar solute and would therefore cause disassociation of the hydrogen-bonded aggregates of the host molecule **13b**. The diffusion coefficient $7.89\times10^{-10}\,m^2s^{-1}$ thus measured in a mixture of $CDCl_3$ and CD_3OD (92:8, v/v) was attributed to the unbound species of **13b** (Figure S7b in the Supporting Information). In $CDCl_3$, however, we observed two distinct diffusion coefficients 6.31×10^{-10} (D_2) and $8.13\times10^{-10}\,m^2s^{-1}$ (D_1), with the latter being slightly higher than $7.89\times10^{-10}\,m^2s^{-1}$ (Figure S7a in the Supporting Information). Because the presence of CD_3OD increases the viscosity of the solution and results in a decrease in the diffusion coefficient, the observed diffusion coefficient $8.13\times10^{-10}\,m^2s^{-1}$ in $CDCl_3$ is most probably attributable to the monomer. On the assumption that the molecules are spherical, the ratio of the molecular weights of the two species calculated from $(D_1/D_2)^3$ is 2.15:1.[15] This indicates that dihydroxylated calix[2]arene[2]triazine **13b** exists in equilibrium with its dimer $(\mathbf{13b})_2$ in $CDCl_3$. The self-association of **13b** was also evidenced by the observation of the $[\mathbf{13b}+H]^+$, $[(\mathbf{13b_2})+H]^+$ and $[(\mathbf{13b})_3+Na]^+$ ion peaks in the ESI mass spectra (Figure S8 in the Supporting Information).

Molecular recognition: The 1,3-alternate dihydroxylated tetraoxacalix[2]arene[2]triazine **13b** contains two hydroxy groups in a V-shaped cleft comprising two conjugated triazine rings. Because the hydroxy group is a hydrogen-bond donor, we envisioned that this functionalised macrocycle would act as a unique host, interacting with guest molecules that are hydrogen-bond acceptors. To demonstrate its utility in molecular recognition, we studied the interaction of **13b** with 1,10-phenanthroline, 4,4′-bipyridine and 2,2′-bipyridine by ^1H NMR titration experiments. As a representative example, the proton NMR spectral changes of **13b** upon addition of an increasing amount of 1,10-phenanthroline are shown in Figure 6. Only one set of proton resonance signals was observed for host **13b** after the addition of the guest, which indicates a fast equilibrium between the host, guest and complex on the NMR spectroscopy timescale. The interaction of the host

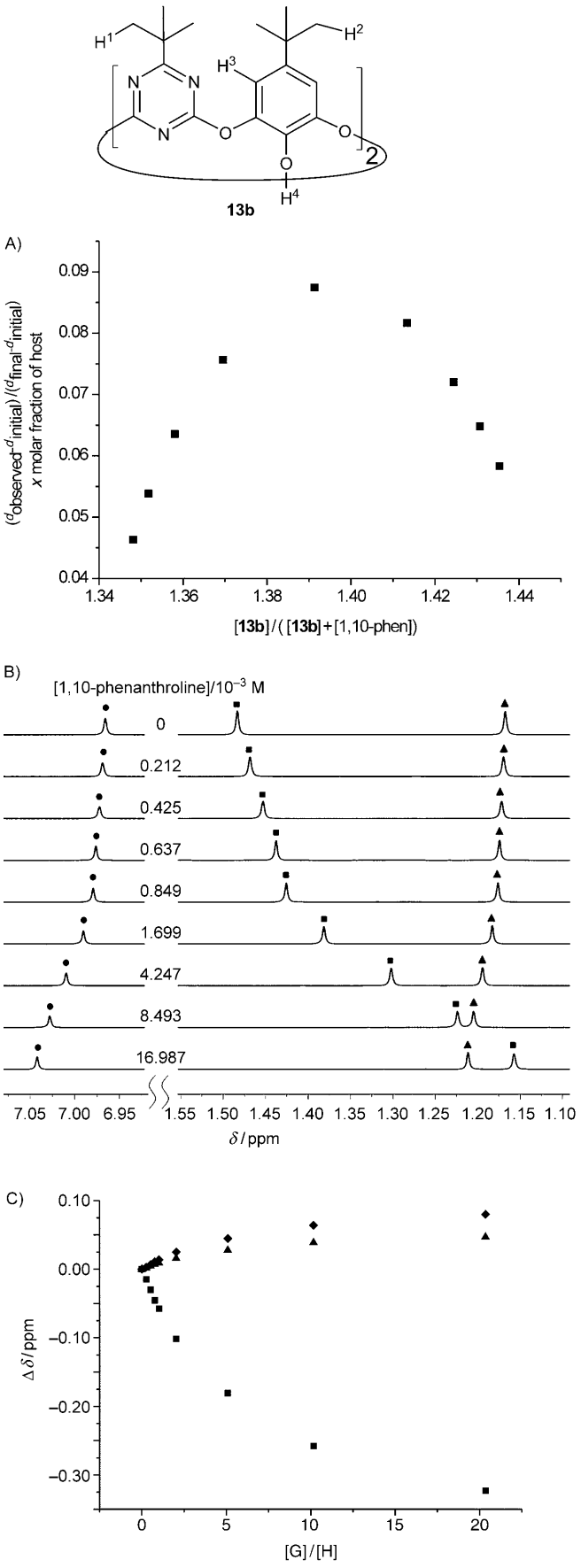

Figure 6. A) Job plot of **13b** and 1,10-phenanthroline. The total concentration of **13b** and 1,10-phenanthroline is 2.0 mM in $CDCl_3$. B) Partial ^1H NMR spectrum of host **13b** (8.35×10^{-4} M) in the presence of an increasing amount of guest 1,10-phenanthroline (0–16.987×10^{-3} M) at 298 K. ■) Peak of H^1, ▲) peak of H^2, ●) peak of H^3. C) NMR titration isotherm. ■) Peak of H^1, ▲) peak of H^2, ◆) peak of H^3. The assignment of protons was determined by NOE experiments.

with the guest led first to a downfield shift and then to the disappearance of the proton signal of the hydroxy group of the host (see Figure S9 in the Supporting information), which indicates the nature of the hydrogen bonding between the host and guest. Interestingly, the proton signals of the benzene ring and the *t*Bu moiety on the benzene ring were shifted downfield, whereas the signal of the *t*Bu on the triazine ring was shifted upfield (Figure 6B). The opposite movements of the two *t*Bu signals reflect the different deshielding and shielding effects experienced by the *t*Bu groups on the benzene and triazine moieties in the presence of the guest molecule. The Job plot in Figure 6A reveals the formation of a 1:1 complex between the host and guest molecules. Based on the NMR titration isotherms (Figure 6C and Figures S11 and S14 in the Supporting Information), association constants between the host and guests, which were fitted by using the Hyperquad 2003 program,[16] are 37.7 M^{-1} for **13b**·2,2′-bipyridine, 200 M^{-1} for **13b**·1,10-phenanthroline and 213 M^{-1} for **13b**·4,4′-bipyridine.

To understand the interaction between the host **13b** and guests on the molecular level, single crystals of the host–guest complexes were cultivated by slow evaporation of solvent from a solution of a mixture of **13b** and the guest. Their structures were analysed by X-ray diffraction analysis and are depicted in Figure 7–9. As expected, the host molecule interacts with all the guest species mainly by forming a hydrogen bond through its hydroxy groups with the nitrogen atoms of the N-heterocycles. Intriguingly, however, the host–guest interaction led to 2+2 complexes in all cases in the solid state. The two dihydroxy-substituted tetraoxacalix[2]arene[2]triazine molecules, which adopt a 1,3-alternate conformation, are aligned head-to-head to form a giant cavity in which two guest molecules are included mainly through the formation of hydrogen bonds.

In the case of the [**13b**·2,2′-bipyridine]$_2$ complex, for example, each of the included *trans*-configured 2,2′-bipyridines forms one strong hydrogen bond with one of the hydroxy groups of one host ($d_{O1-N8}=2.694$ Å) and one relatively weak hydrogen bond with one of the hydroxy groups of the other host ($d_{O2-N7}=2.896$ Å). In the middle of the cavity, two pyridine rings of two guests are parallel displaced with a face-to-face distance of 3.451 Å (Figure 7). Figure 8 shows that in the complex of **13b** with 4,4′-bipyridine, two guest molecules simply act as two bridges to link two host molecules through the formation of two pairs of intermolecular hydrogen bonds ($d_{O5-N8}=2.731$ Å and $d_{O6-N7}=2.696$ Å). Although there is no π–π interaction between the two guest molecules, the shorter distance between the aromatic carbon C41 of one 4,4′-bipyridine molecule and the aromatic plane

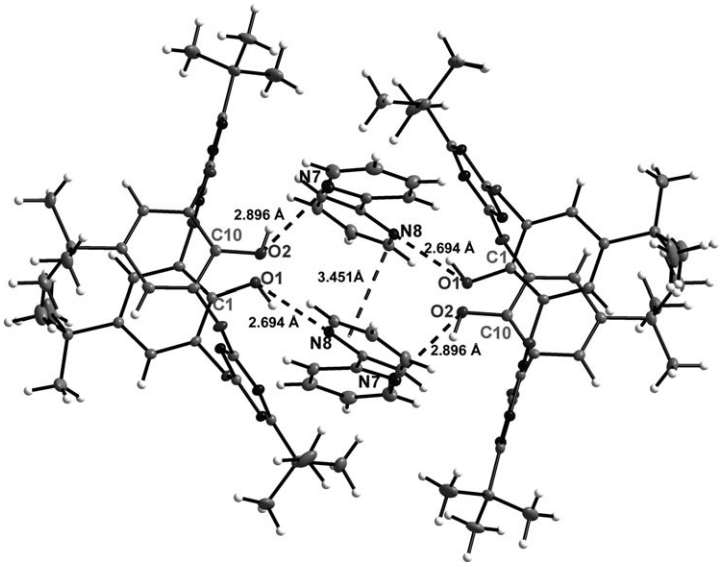

Figure 7. Molecular structure of the complex formed between host **13b** and 2,2′-bipyridine. Selected interaction distances [Å]: O1···N8 2.694, O2···N7 2.896, pyridine rings π–π 3.451. Selected hydrogen-bonding angles [°]: O1–H···N8 153.1, O2–H···N7 144.9.

of the other molecule [$d_{C41-pyridine\ ring}=3.328$ Å] suggests $C41_{aromatic}$–H41A···π interactions. The multiple non-covalent bond interactions in the complex of [**13b**·1,10-phenanthroline]$_2$ are worth noting. First, one of the hydroxy groups of the host forms an intermolecular hydrogen bond with one nitrogen atom of 1,10-phenanthroline ($d_{O6-N7}=2.648$ Å). The other hydroxy group is probably intramolecularly hydrogen bonded to an adjacent triazine nitrogen ($d_{O5-N6}=3.013$ Å). In addition, weak C–H···π (C39–H39···C31) and hydrogen-bonding (C43–H43···O5) interactions are observed. Furthermore, one of the *t*Bu groups of the host interacts with the guest through a C–H···π interaction with the distance between C12 and the plane of the 1,10-phenanthroline being 3.601 Å. In addition to the intermolecular hydrogen bonds, a lone-pair-electron–π interaction between 1,10-phenanthroline and triazine of the host in [**13b**·1,10-phenanthroline]$_2$ is also observed with the distances between N8 and the plane and the centroid of the triazine being 3.317 and 3.311 Å, respectively (Figure 9). Moreover, two guest molecules are π–π displaced stacked and the distance between two anti-face-to-face parallel 1,10-phenanthroline planes is 3.481 Å.

Note that although the dihydroxylated tetraoxacalix[2]arene[2]triazine host **13b** retains almost the same 1,3-alternate

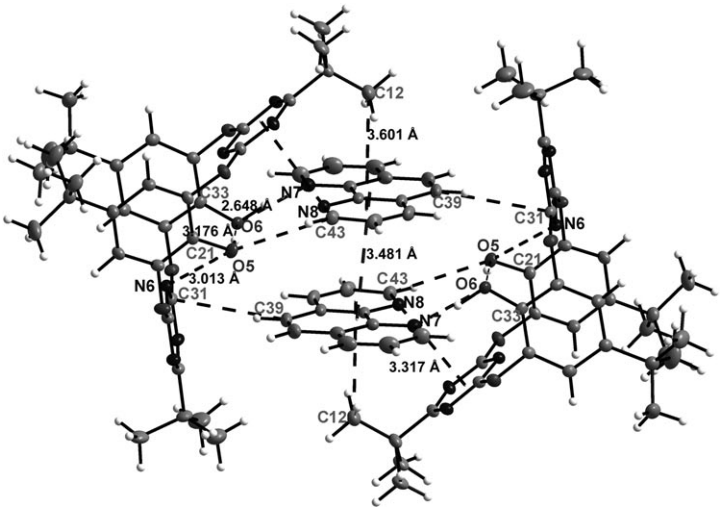

Figure 9. Molecular structure of the complex formed between host **13b** and 1,10-phenanthroline. Selected interaction distances [Å]: O6···N7 2.648, O5···O6 3.176, N8···triazine plane 3.317, C12–H···π 3.601, π–π stacking distance between 1,10-phenanthroline planes 3.481. Selected hydrogen-bonding angles [°]: O6–H···N7 154.7, O5–H···O6 173.0.

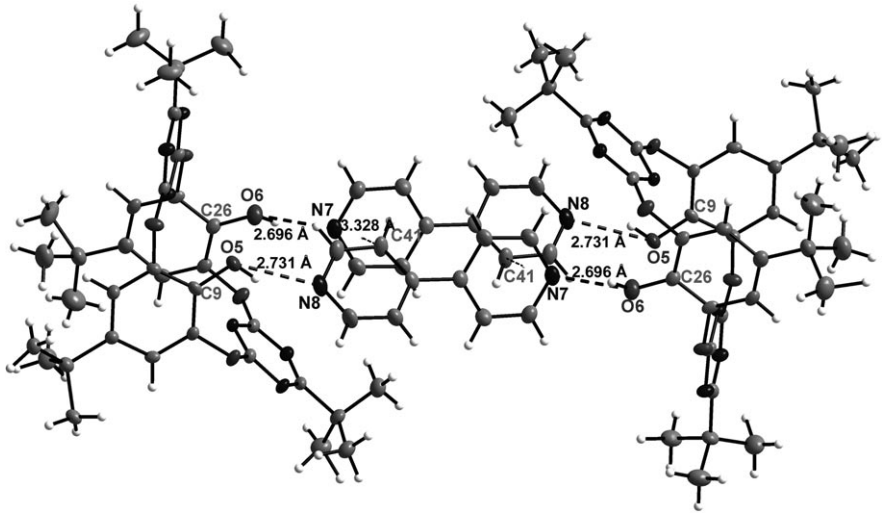

Figure 8. Molecular structure of the complex formed between host **13b** and 4,4′-bipyridine. Selected interaction distances [Å]: O6···N7 2.696, O5···N8 2.731, C41–H···π 3.328. Selected hydrogen-bonding angles [°]: O6–H···N7 159.6, O5–H···N8 153.0.

conformation in the complex structures (Figures 7–9), careful scrutiny of the host molecule structures in the three complexes reveals that the cavity size varies according to the guest molecule included. The upper rim distance between two triazine rings, a parameter defining the size of the tetraoxacalix[2]arene[2]triazine macrocycles, differs from 9.516 Å for [**13b**·2,2′-bipyridine]$_2$ to 9.385 Å for [**13b**·4,4′-bipyridine]$_2$ and to 9.285 Å for [**13b**·1,10-phenanthroline]$_2$. These values contrast with the upper rim distance between two triazine rings of the parent macrocycle **13b** of 9.022 Å (Figure 4). It is appa-

rently the guest species that induces the host to change its cavity size during complexation. Nevertheless, it is the oxygen bridges of the tetraoxacalix[2]arene[2]triazine that regulate their conjugation with the aromatic rings, leading to fine-tuning of the cavity to achieve the best fit with the guest molecules. The formation of 1+1 complexes between the host and guests examined probably did not occur because of the short distance between the two nitrogen atoms, the hydrogen-bond acceptors, of the guest molecule. Such a short distance is energetically unfavourable for the formation of two hydrogen bonds with the hydroxy groups.

Conclusion

We have established a simple method for the construction of functionalised tetraoxacalix[2]arene[2]triazine macrocycles by the fragment coupling approach using 1,2,3-trihydroxybenzene derivatives as the starting materials under very mild conditions. Although a mixture of monomer and dimer was observed in solution through a diffusion NMR study, the lower-rim-dihydroxylated tetraoxacalix[2]arene[2]triazine **13b** adopts a 1,3-alternate conformation and forms a cyclic tetrameric assembly in the solid state as a result of the formation of an intermolecular hydrogen-bond network. The dihydroxylated macrocyclic host molecule acts as a hydrogen-bond donor to interact with 2,2′-bipyridine, 4,4′-bipyridine and 1,10-phenanthroline guests. Whereas they form in solution the corresponding 1:1 complexes with binding constants ranging from 37.7 to 213 M^{-1}, in the crystalline state 2+2 complexes were furnished between the host and the guest. X-ray crystallography convincingly revealed that it is predominantly the hydrogen-bonding interactions that bring the host and guest molecules together. In addition, non-covalent interactions such as lone-pair-electron–π and C–H···π interactions also contribute to the stabilisation of the host–guest complexes.

Experimental Section

Preparation of methyl benzoates 5a–c: A solution of methyl 4-alkoxy-3,5-dihydroxybenzoate (**4a–c**; 10 mmol) and diisopropylethylamine (3.23 g, 25 mmol) in THF (40–200 mL) was added dropwise to an ice-bath-cooled solution of cyanuric chloride (**2**; 4.06 g, 22 mmol) in THF (60–150 mL) over 1–2 h. A white solid was precipitated from the reaction solution. The resulting mixture was stirred for another 2 h at 0 °C. After filtration, the filtrate was concentrated under reduced pressure and the residue purified by chromatography using a silica gel column eluted with a mixture of petroleum ether and ethyl acetate.

*Methyl 3,5-bis(4,6-dichloro-1,3,5-triazin-2-yloxy)-4-(vinyloxy)benzoate (**5a**)*: White solid; m.p. 112–113 °C; ^{1}H NMR (300 MHz, $CDCl_3$, 25 °C, TMS): δ = 7.90 (s, 2H), 5.82–5.69 (m, 1H), 5.13 (d, J = 3.5 Hz, 1H), 5.09 (s, 1H), 4.53 (d, J = 5.7 Hz, 2H), 3.95 ppm (s, 3H); ^{13}C NMR (75 MHz, $CDCl_3$, 25 °C, TMS): δ = 173.3, 170.7, 164.5, 146.2, 144.6, 131.8, 126.6, 122.6, 118.7, 75.0, 52.7 ppm; IR (KBr): $\tilde{\nu}$ = 1727, 1620, 1529 cm^{-1}; MS (EI): *m/z* (%): 522 (3), 521 (1), 520 (6), 519 (1), 518 (5) $[M]^+$, 356 (5), 354 (7), 87 (6), 41 (100), 32 (32); elemental analysis calcd (%) for $C_{17}H_{10}N_6O_5Cl_4$: C 39.26, H 1.94, N 16.16; found: C 39.15, H 2.00, N 16.12.

*Methyl 4-(benzyloxy)-3,5-bis(4,6-dichloro-1,3,5-triazin-2-yloxy)benzoate (**5b**)*: White solid; m.p. 173–174 °C; ^{1}H NMR (300 MHz, $CDCl_3$, 25 °C, TMS): δ = 7.88 (s, 2H), 7.29–7.25 (m, 3H), 7.15–7.11 (m, 2H), 5.08 (s, 2H), 3.94 ppm (s, 3H); ^{13}C NMR (75 MHz, $CDCl_3$, 25 °C, TMS): δ = 173.2, 170.6, 164.5, 146.3, 144.4, 135.1, 128.7, 128.5, 127.3, 126.4, 122.7, 76.1, 52.7 ppm; IR (KBr): $\tilde{\nu}$ = 1730, 1524 cm^{-1}; MS (EI): *m/z* (%): 574 (1), 572 (2), 570 (3), 568 (3) $[M]^+$, 91 (100); elemental analysis calcd (%) for $C_{21}H_{12}N_6O_5Cl_4$: C 44.24, H 2.12, N 14.74; found: C 44.56, H, 2.11, N 14.87.

*Methyl 3,5-bis(4,6-dichloro-1,3,5-triazin-2-yloxy)-4-methoxybenzoate (**5c**)*: White solid; m.p. 110–112 °C; ^{1}H NMR (300 MHz, $CDCl_3$, 25 °C, TMS): δ = 7.89 (s, 2H), 3.94 (s, 3H), 3.82 ppm (s, 3H); ^{13}C NMR (75 MHz, $CDCl_3$, 25 °C, TMS): δ = 173.3, 170.6, 164.5, 147.5, 144.3, 126.4, 122.7, 61.9, 52.8; IR (KBr): $\tilde{\nu}$ = 1727, 1621, 1529 cm^{-1}; MS (EI): *m/z* (%): 498 (4), 497 (3), 496 (16), 495 (6), 494 (36), 493 (5), 492 (26) $[M]^+$, 465 (33), 464 (12), 463 (71), 462 (16), 461 (77), 460 (21), 459 (100), 458 (20), 457 (99); elemental analysis calcd (%) for $C_{15}H_8Cl_4N_6O_5$: C 36.46, H 1.63, N 17.01; found: C 36.68, H 1.90, N 16.89.

General procedure for the synthesis of tetraoxacalix[2]arene[2]triazine derivatives 6a–c: Acetone (250 mL) solutions of linear trimer **5c** (0.79 g, 1.6 mmol) and methyl 4-methoxy-3,5-dihydroxybenzoate (**4c**; 0.317 g, 1.6 mmol) were added dropwise at the same rate to a well-stirred solution of diisopropylethylamine (0.50 g, 3.84 mmol) in acetone (200 mL) at room temperature over 8–12 h. The resulting reaction mixture was stirred for another 2 days at room temperature. After removal of the solvent under reduced pressure, the residue was subjected to silica gel chromatography eluting with a mixture of petroleum ether and dichloromethane to give pure products.

*Compound **6a***: M.p. 293–295 °C; ^{1}H NMR (300 MHz, $CDCl_3$, 25 °C, TMS): δ = 7.64 (s, 4H), 5.84–5.71 (m, 2H), 5.12 (s, 2H), 5.07 (d, J = 7.1 Hz, 2H), 4.42 (d, J = 5.6 Hz, 4H), 3.89 ppm (s, 6H); ^{13}C NMR (75 MHz, $CDCl_3$, 25 °C, TMS): δ = 174.3, 171.8, 164.6, 146.1, 144.7, 131.9, 126.2, 122.1, 118.7, 74.8, 52.6 ppm; IR (KBr): $\tilde{\nu}$ = 1731, 1651, 1622, 1551 cm^{-1}; MS (MALDI-TOF): *m/z* (%): 671.6 (100) $[M+1]^+$, 672.6 (36), 673.6 (77), 674.6 (24), 675.6 (17); elemental analysis calcd (%) for $C_{28}H_{20}N_6O_{10}Cl_2$: C 50.09, H 3.00, N 12.52; found: C 50.21, H 3.05, N 12.40.

*Compound **6b***: M.p. 230–232 °C; ^{1}H NMR (300 MHz, $CDCl_3$, 25 °C, TMS): δ = 7.62 (s, 4H), 7.30–7.19 (m, 6H), 7.08–7.04 (m, 4H), 4.89 (s, 4H), 3.88 ppm (s, 6H); ^{13}C NMR (75 MHz, $CDCl_3$, 25 °C, TMS): δ = 174.2, 171.7, 164.6, 146.2, 144.6, 135.1, 128.7, 128.4, 127.7, 126.1, 122.1, 76.1, 52.6 ppm; IR (KBr): $\tilde{\nu}$ = 1727, 1603, 1550 cm^{-1}; MS (MALDI-TOF): *m/z* (%): 771.2 (18) $[M+1]^+$, 772.2 (10), 773.2 (15), 774.2 (6), 793.2 (100) $[M+Na]^+$, 794.2 (40), 795.2 (65), 796.2 (23), 797.2 (15); elemental analysis calcd (%) for $C_{36}H_{24}N_6O_{10}Cl_2$: C 56.04, H 3.14, N 10.89; found: C 56.20, H 3.09, N 10.91.

*Compound **6c***: M.p. >300 °C; ^{1}H NMR (300 MHz, $CDCl_3$, 25 °C, TMS): δ = 7.62 (s, 4H), 3.88 (s, 6H), 3.75 ppm (s, 6H); ^{13}C NMR (75 MHz, $CDCl_3$, 25 °C, TMS): δ = 174.5, 171.9, 164.5, 147.7, 144.3, 125.9, 122.4, 61.8, 52.6 ppm; IR (KBr): $\tilde{\nu}$ = 1733, 1622, 1553 cm^{-1}; MS (FAB): *m/z* (%): 618 (93) $[M]^+$, 619 (100), 620 (66), 621 (37), 622 (24); elemental analysis calcd (%) for $C_{26}H_{16}N_6O_{10}Cl_2$: C 46.54, H 2.60, N 13.57; found: C 46.35, H 2.61, N 13.35.

*Compound **7a***: M.p. >300 °C; ^{1}H NMR (300 MHz, $CDCl_3$, 25 °C, TMS): δ = 7.70 (s, 6H), 5.70–5.59 (m, 3H), 5.11–4.94 (m, 6H), 4.43 (d, J = 3.8 Hz, 6H), 3.88 ppm (s, 9H); ^{13}C NMR (75 MHz, $CDCl_3$, 25 °C, TMS): δ = 173.8, 171.6, 164.6, 147.1, 144.1, 132.2, 125.9, 122.1, 117.0, 73.8, 52.6 ppm; IR (KBr): $\tilde{\nu}$ = 1727, 1620, 1553 cm^{-1}; MS (MALDI-TOF): *m/z* (%): 1006.2 (44) $[M+1]^+$, 1007.2 (26), 1008.2 (50), 1009.2 (19), 1010.2 (23), 1028.2 (73) $[M+Na]^+$, 1029.2 (36), 1030.2 (100), 1031.2 (41), 1032.2 (39); elemental analysis calcd (%) for $C_{42}H_{30}N_9O_{15}Cl_3$: C 50.09, H 3.00, N 12.52; found: C 50.01, H 3.00, N 12.28.

*Compound **7c***: M.p. >300 °C; ^{1}H NMR (300 MHz, $CDCl_3$, 25 °C, TMS): δ = 7.68 (s, 6H), 3.88 (s, 9H), 3.73 ppm (s, 9H); ^{13}C NMR (75 MHz, $CDCl_3$, 25 °C, TMS): δ = 174.0, 171.9, 164.6, 147.9, 143.8, 125.5, 122.3, 61.4, 52.6 ppm; IR (KBr): $\tilde{\nu}$ = 1727, 1622, 1551 cm^{-1}; MS (MALDI-TOF): *m/z* (%): 950.2 (90) $[M+Na]^+$, 951.2 (33), 952.2 (100), 953.2 (37), 954.2

(32); elemental analysis calcd (%) for $C_{36}H_{24}N_9O_{15}Cl_3$: C 46.54, H 2.60, N 13.57; found: C 46.59, H 2.71, N 13.34.

Synthesis of 12a from 6b: A solution of **6b** (386 mg, 0.5 mmol) in THF (20 mL) was added dropwise to a solution of di-*n*-propylamine (121 mg, 1.2 mmol) and diisopropylethylamine (284 mg, 2.2 mmol) in THF (20 mL) at reflux over 30 min. After heating at reflux for another 6.5 h, the reaction was stopped. The reaction mixture was then concentrated and the residue was purified by chromatography on a silica gel column eluting with a mixture of petroleum ether and ethyl acetate to afford pure product **12a**. M.p. 160–161 °C; ^{1}H NMR (300 MHz, $CDCl_3$, 25 °C, TMS): $\delta = 7.50$ (s, 4H), 7.13–7.03 (m, 10H), 4.89 (s, 4H), 3.84 (s, 6H), 3.64–3.45 (m, 8H), 1.65 (hex., $J = 7.3$ Hz, 8H), 0.95 ppm (t, $J = 7.3$ Hz, 12H); ^{13}C NMR (75 MHz, $CDCl_3$, 25 °C, TMS): $\delta = 171.6$, 167.6, 165.4, 147.8, 145.1, 136.6, 128.0, 127.6, 127.4, 124.7, 122.2, 74.8, 52.2, 49.4, 20.8, 11.4 ppm; IR (KBr): $\tilde{\nu} = 1727$, 1605, 1577 cm^{-1}; MS (MALDI-TOF): *m/z* (%): 901.4 $[M+1]^+$, 923.4 $[M+Na]^+$, 939.4 $[M+K]^+$; elemental analysis calcd (%) for $C_{48}H_{52}N_8O_{10}$: C 63.99, H 5.82, N 12.44; found: C 63.69, H 5.59, N 12.49.

General procedure for the synthesis of the lower-rim-dihydroxylated tetraoxacalix[2]arene[2]triazines 11 and 13a,b: Under argon at room temperature, anhydrous $AlCl_3$ (2.0 g, 15 mmol) and dried toluene (100 mL) were mixed together and stirred for 5–30 min. Macrocycle **6a**, **6b**, **12a** or **12b** (0.5 mmol) was then added and the resulting mixture was stirred at room temperature for 0.5–12 h. The reaction mixture was then poured into a mixture of crushed ice and water (100 mL) and dilute hydrochloric acid (10%, 15 mL) was added. The organic layer was separated and the aqueous layer extracted twice with ethyl acetate (2×150 mL). The combined organic layers was dried over anhydrous sodium sulfate and concentrated under vacuum. Crystallisation of the residue from a mixture of hexane and dichloromethane gave pure product **13a**, whereas pure **11** and **13b** were isolated by silica gel chromatography using a mixture of petroleum ether and ethyl acetate as eluent.

*Compound **11***: M.p. >300 °C; ^{1}H NMR (300 MHz, [D$_6$]DMSO, 25 °C, TMS): $\delta = 10.87$ (s, OH, 2H), 8.39 (d, $J = 8.2$ Hz, 4H), 7.50 (s, 4H), 7.45 (d, $J = 8.2$ Hz, 4H), 3.74 (s, 6H), 2.45 ppm (s, 6H); ^{13}C NMR (75 MHz, [D$_6$]DMSO, 25 °C, TMS): $\delta = 175.2$, 172.1, 164.6, 147.0, 143.9, 140.1, 131.5, 129.7, 128.7, 121.7, 119.2, 51.9, 21.2 ppm; IR (KBr): $\tilde{\nu} = 3604$, 3459, 1703, 1623, 1577, 1568 cm^{-1}; MS (ESI, neg.): *m/z* (%): 701.1 $[M-1]^+$; elemental analysis calcd (%) for $C_{36}H_{26}N_6O_{10}$: C 61.54, H 3.73, N 11.96; found: C 61.31, H 3.96, N 11.95.

*Compound **13a***: M.p. 238–240 °C; ^{1}H NMR (300 MHz, $CDCl_3$, 25 °C, TMS): $\delta = 7.55$ (s, 4H), 5.62 (s, OH, 2H), 3.83 (s, 6H), 3.63–3.50 (m, 8H), 1.70 (hex., $J = 7.5$ Hz, 8H), 0.96 ppm (t, $J = 7.4$ Hz, 12H); ^{13}C NMR (300 MHz, [D$_6$]DMSO, 25 °C, TMS): $\delta = 10.34$ (s, OH, 2H), 7.27 (s, 4H), 3.72 (s, 6H), 3.56–3.51 (m, 8H), 1.65 (hex., $J = 7.3$ Hz, 8H), 0.92 ppm (t, $J = 7.3$ Hz, 12H); ^{13}C NMR (75 MHz, $CDCl_3$, 25 °C, TMS): $\delta = 171.0$, 167.4, 165.4, 145.0, 140.8, 122.4, 121.8, 52.2, 49.5, 20.8, 11.2 ppm; IR (KBr): $\tilde{\nu} = 3355$, 1724, 1705, 1612, 1592 cm^{-1}; MS (MALDI-TOF): *m/z* (%): 721.9 $[M+1]^+$, 743.9 $[M+Na]^+$, 759.8 $[M+K]^+$; elemental analysis calcd (%) for $C_{34}H_{40}N_8O_{10}$: C 56.66, H 5.59, N 15.55; found: C 56.36, H 5.51, N 15.43.

*Compound **13b***: M.p. 210–212 °C; ^{1}H NMR (300 MHz, $CDCl_3$, 25 °C, TMS): $\delta = 6.91$ (s, 4H), 5.75 (s, OH, 2H), 1.38 (s, 18H), 1.13 ppm (s, 18H); ^{13}C NMR (75 MHz, $CDCl_3$, 25 °C, TMS): $\delta = 191.8$, 171.6, 145.8, 141.8, 136.8, 116.5, 39.6, 34.3, 31.0, 28.6 ppm; IR (KBr): $\tilde{\nu} = 3652$, 3399, 3188, 1622, 1575, 1548 cm^{-1}; MS (ESI, pos.): *m/z* (%): 631.5 $[M+1]^+$, 653.4 $[M+Na]^+$, 669.4 $[M+K]^+$; elemental analysis calcd (%) for $C_{34}H_{42}N_6O_6$: C 64.74, H 6.71, N 13.32; found: C 64.65, H 7.13, N 13.50.

^{1}H NMR spectral titrations: In each ^{1}H NMR titration experiment, the concentration of host **13b** was kept constant and the concentration of guest was increased gradually from 0–16.987×10^{-3} M for 1,10-phenanthroline, 0–33.72×10^{-3} M for 4,4′-bipyridine and 0–34.00×10^{-3} M for 2,2′-bipyridine. The stoichiometry of the complex was obtained by the Job plot method. The association constants were calculated on the basis of ^{1}H NMR experimental isotherms using Hyperquad 2003 program.

Preparation of single crystals: The single crystals of **6a**, **6b**, **7a**, and **14** suitable for X-ray analysis were obtained by slow evaporation of a solution of dichloromethane and hexane at room temperature. Slow evaporation of a mixture of diethyl ether and hexane gave a single crystal of **13b** suitable for X-ray analysis. Single crystals of the complexes were obtained by slow evaporation of solutions of **13b** (10 mg) and 2,2′-bipyridine (10 mg) in dichloromethane and hexane, **13b** (10 mg) and 4,4′-bipyridine (10 mg) in acetone and hexane, and **13b** (10 mg) and 1,10-phenanthroline (10 mg) in dichloromethane and hexane, respectively.

CCDC-759599 (**6a**), 759852 (**7a**), 759949 (**13b**·0.25 hexane·$H_2$0), 759950 (**14**), 759951 (**13b**·1,10-phen), 759952 (**13b**·4,4′-bipy) and 759953 (**13b**·2,2′-bipy) contain the supplementary crystallographic data for this paper. These data can be obtained free of charge from The Cambridge Crystallographic Data Centre via www.ccdc.cam.ac.uk/data_request/cif.

Acknowledgements

We thank the National Science Foundation of China (NSFC, 20532030), the Ministry of Science and Technology (MOST, 2007CB808005) and the Chinese Academy of Sciences (CAS) for financial support. We also thank Dr. X. Hao and T.-L. Liang for X-ray structure determination and Dr. J.-F. Xiang for NMR measurements and discussions.

[1] C. J. Pedersen, *J. Am. Chem. Soc.* **1967**, *89*, 7017–7036.
[2] D. J. Cram, *Angew. Chem.* **1986**, *98*, 1041–1060; *Angew. Chem. Int. Ed. Engl.* **1986**, *25*, 1039–1057.
[3] B. Dietrich, J.-M. Lehn, J. P. Sauvage, *Tetrahedron Lett.* **1969**, *10*, 2885–2888.
[4] a) *Calixarenes* (Eds.: Z. Asfari, V. Böhmer, J. Harrowfield, J. Vicens, M. Saadioui), Kluwer Academic, Dordrecht, **2001**; b) C. D. Gutsche, *Calixarenes Revisited*, RSC, Cambridge, **1998**; c) *Calixarenes in Action* (Eds.: L. Mandolini, R. Ungaro), Imperial College Press, London, **2000**; d) G. J. Lumetta, R. D. Rogers, A. S. Gopalan, *Calixarenes for Separation*, ACS, Washington, **2000**.
[5] For a monograph, see: C. D. Gutsche, *Calixarenes*, RSC, Cambridge, **1989**.
[6] For useful reviews on heterocalixaromatics, see: a) M.-X. Wang, *Chem. Commun.* **2008**, *4541*–4551; b) W. Maes, W. Dehaen, *Chem. Soc. Rev.* **2008**, *37*, 2393–2402; c) H. Tsue, K. Ishibashi, R. Tamura, *Top. Heterocycl. Chem.* **2008**, *17*, 73–96; d) B. König, M. H. Fonseca, *Eur. J. Inorg. Chem.* **2000**, 2303–2310.
[7] For recent examples of nitrogen-bridged calixaromatics, see: a) A. Ito, Y. Ono, K. Tanaka, *New J. Chem.* **1998**, *22*, 779–781; b) A. Ito, Y. Ono, K. Tanaka, *J. Org. Chem.* **1999**, *64*, 8236–8241; c) Y. Miyazaki, T. Kanbara, T. Yamamoto, *Tetrahedron Lett.* **2002**, *43*, 7945–7948; d) M.-X. Wang, X.-H. Zhang, Q.-Y. Zheng, *Angew. Chem.* **2004**, *116*, 856–860; *Angew. Chem. Int. Ed.* **2004**, *43*, 838–842; e) H.-Y. Gong, X.-H. Zhang, D.-X. Wang, H.-W. Ma, Q.-Y. Zheng, M.-X. Wang, *Chem. Eur. J.* **2006**, *12*, 9262–9275; f) H.-Y. Gong, Q.-Y. Zheng, X.-H. Zhang, D.-X. Wang, M.-X. Wang, *Org. Lett.* **2006**, *8*, 4895–4898; g) H. Tsue, K. Ishibashi, H. Takahashi, R. Tamura, *Org. Lett.* **2005**, *7*, 2165–2168; h) W. Fukushima, T. Kanbara, T. Yamamoto, *Synlett* **2005**, 2931–2934; i) T. D. Selby, S. C. Blackstock, *Org. Lett.* **1999**, *1*, 2053–2055; j) Y. Suzuki, T. Yanagi, T. Kanbara, T. Yamamoto, *Synlett* **2005**, 263–266; k) K. Ishibashi, H. Tsue, S. Tokita, K. Matsui, H. Takahashi, R. Tamura, *Org. Lett.* **2006**, *8*, 5991–5994; l) H.-Y. Gong, D.-X. Wang, J.-F. Xiang, Q.-Y. Zheng, M.-X. Wang, *Chem. Eur. J.* **2007**, *13*, 7791–7802; m) S.-Q. Liu, D.-X. Wang, Q.-Y. Zheng, M.-X. Wang, *Chem. Commun.* **2007**, *3856*–3858; n) E.-X. Zhang, D.-X. Wang, Q.-Y. Zheng, M.-X. Wang, *Org. Lett.* **2008**, *10*, 2565–2568; o) H.-Y. Gong, D.-X. Wang, Q.-Y. Zheng, M.-X. Wang, *Tetrahedron* **2009**, *65*, 87–92; p) J. Clayden, S. J. M. Rowbottom, W. J. Ebenezer, M. G. Hutchings, *Org. Biomol. Chem.* **2009**, *7*, 4871–4880; q) M. Xue, C. F. Chen, *Org. Lett.* **2009**, *11*, 5294–5297; r) H. Konishi, S. Hashimoto, T. Sakakibara, S. Matsubara, Y. Yasukawa, O. Morikawa, K. Kobayashi, *Tetrahedron Lett.* **2009**, *50*, 620–623.

[8] For recent examples of oxygen-bridged calixaromatics, see: a) M.-X. Wang, H.-B. Yang, *J. Am. Chem. Soc.* **2004**, *126*, 15412–15422; b) J. L. Katz, M. B. Feldman, R. R. Conry, *Org. Lett.* **2005**, *7*, 91–94; c) J. L. Katz, K. J. Selby, R. R. Conry, *Org. Lett.* **2005**, *7*, 3505–3507; d) J. L. Katz, B. J. Geller, R. R. Conry, *Org. Lett.* **2006**, *8*, 2755–2758; e) W. Maes, W. Van Rossom, K. Van Hecke, L. Van Meervelt, W. Dehaen, *Org. Lett.* **2006**, *8*, 4161–4164; f) E. Hao, F. R. Fronczek, M. G. H. Vicente, *J. Org. Chem.* **2006**, *71*, 1233–1236; g) R. D. Chambers, P. R. Hoskin, A. R. Kenwright, A. Khalil, P. Richmond, G. Sandford, D. S. Yufit, J. A. K. Howard, *Org. Biomol. Chem.* **2003**, *1*, 2137–2147; h) R. D. Chambers, P. R. Hoskin, A. Khalil, P. Richmond, G. Sandford, D. S. Yufit, J. A. K. Howard, *J. Fluorine Chem.* **2002**, *116*, 19–22; i) X. H. Li, T. G. Upton, C. L. D. Gibb, B. C. Gibb, *J. Am. Chem. Soc.* **2003**, *125*, 650–651; j) F. Yang, L.-W. Yan, K.-Y. Ma, L. Yang, J.-H. Li, L.-J. Chen, J.-S. You, *Eur. J. Org. Chem.* **2006**, 1109–1112; k) Q.-Q. Wang, D.-X. Wang, Q.-Y. Zheng, M.-X. Wang, *Org. Lett.* **2007**, *9*, 2847–2850; l) J. L. Katz, B. J. Geller, P. D. Foster, *Chem. Commun.* **2007**, 1026–1028; m) C. Zhang, C.-F. Chen, *J. Org. Chem.* **2007**, *72*, 3880–3888; n) W. Van Rossom, W. Maes, L. Kishore, M. Ovaere, L. Van Meervelt, W. Dehaen, *Org. Lett.* **2008**, *10*, 585–588; o) M. Li, M. L. Ma, X. Y. Li, K. Wen, *Tetrahedron* **2009**, *65*, 4639–4643; p) W. Van Rossom, M. Ovaere, L. Van Meervelt, W. Dehaen, W. Maes, *Org. Lett.* **2009**, *11*, 1681–1684; q) S. Akagi, Y. Yasukawa, K. Kobayashi, H. Konishi, *Tetrahedron* **2009**, *65*, 9983–9988.

[9] For a review on thiacalixarenes, see: N. Morohashi, F. Narumi, N. Iki, T. Hattori, S. Miyano, *Chem. Rev.* **2006**, *106*, 5291–5316.

[10] For examples of other heteroatom-bridged calixaromatics, see: a) B. Koenig, M. Rödel, P. Bubenitschek, P. G. Jones, I. Thondorf, *J. Org. Chem.* **1995**, *60*, 7406–7410; b) B. König, M. Rödel, P. Bubenitschek, P. G. Jones, *Angew. Chem.* **1995**, *107*, 752–754; *Angew. Chem. Int. Ed. Engl.* **1995**, *34*, 661–662; c) M. Yoshida, M. Goto, F. Nakanishi, *Organometallics* **1999**, *18*, 1465–1470; d) N. Avarvari, N. Mezailles, L. Ricard, P. Le Floch, F. Mathey, *Science* **1998**, *280*, 1587–1589; e) N. Avarvari, N. Maigrot, L. Ricard, F. Mathey, P. Le Floch, *Chem. Eur. J.* **1999**, *5*, 2109–2118.

[11] D.-X. Wang, Q.-Y. Zheng, Q.-Q. Wang, M.-X. Wang, *Angew. Chem.* **2008**, *120*, 7595–7598; *Angew. Chem. Int. Ed.* **2008**, *47*, 7485–7488.

[12] B.-Y. Hou, D.-X. Wang, H.-B. Yang, Q.-Y. Zheng, M.-X. Wang, *J. Org. Chem.* **2007**, *72*, 5218–5226.

[13] W. Maes, W. V. Rossom, K. V. Hecke, L. V. Meervelt, W. Dehaen, *Org. Lett.* **2006**, *8*, 4161–4164.

[14] a) H. Kämmerer, G. Happel, V. Böhmer, D. Rathay, *Monatsh. Chem.* **1978**, *109*, 767–773; b) C. D. Gutsche, J. A. Levine, *J. Am. Chem. Soc.* **1982**, *104*, 2652–2653.

[15] C. Schalley, *Analytical Methods in Supramolecular Chemistry*, Wiley-VCH, Weinheim, **2007**, p. 193.

[16] a) P. Gans, A. Sabatini, A. Vacca, *Talanta* **1996**, *43*, 1739–1753; b) Hyperquad 2003 software, Protonic Software, http://www.hyperquad.co.uk.

Received: January 4, 2010
Published online: May 12, 2010

